

Flexible operation strategy for geothermal power generation adapted to the uncertainty of demand response

Jingxuan Xie , Jiansheng Wang *

Key Laboratory of Efficient Utilization of Low and Medium Grade Energy, MOE, School of Mechanical Engineering, Tianjin University, Tianjin, 300350, P. R. China

(*Corresponding Author: jsw@tju.edu.cn)

ABSTRACT

Flexible operation of enhanced geothermal system (EGS) can not only address the peak modulation of geothermal power generation, but also actually improve the utilization of geothermal resource. Thus, an inversion investigation is presented to explore the effect of the flexible operation of EGS on reservoir lifespan using a pinnate horizontal well in present work. A nested iterative program is developed to fit the relationship between the generation capacity and operation time first, and injection flow rate second, by incorporating the non-linear least squares and Levenberg-Marquardt method. Particle swarm optimization (PSO) with self-adaptive inertia weight algorithm is employed to inverse the flexible operation strategy according to the surrogate model and the data of power consumption in demand side. The result indicates that the generation capacity and production temperature of EGS with pinnate horizontal well are strongly associated only with the injection mass flow rate. According to the power consumption in demand side, the geothermal power plant proposed should be launched at spring or autumn to avoid the geothermally seismic activity that caused by the larger injection flow rate. The flexible operation strategy of EGS with pinnate horizontal well should be implemented 11.25 days earlier than expected. Compared with the optimum operation strategy, the application of flexible operation strategy delays the thermal breakthrough time by 1.28 years, but causes a higher pump consumption.

Keywords: Geothermal power generation, Flexible operation strategy, Inversion analysis, Enhanced geothermal system

NONMENCLATURE

Abbreviations

EGS	Enhanced geothermal system
HDR	Hot dry rock
PSO	Particle swarm optimization
NSGAI	Non-dominated Sorting Genetic Algorithm II
TOPSIS	Technique of Order Preference by Similarity to Ideal Solution

Symbols

w	Inertia weight coefficient
f	Average value
η_{ex}	Exergy efficiency
m	Mass flow rate
inj	Injection well
pro	Production well
h	Enthalpy
T	Temperature
E	Output power
$a, b, c \text{ and } d$	Undetermined coefficient
E_p	Power demand
t	Secs

1. INTRODUCTION

Enhanced geothermal system (EGS) has been become an efficient method to develop the geothermal resource of hot dry rock (HDR). However, the generating capacity and service life of EGS were significantly affected by the operation strategies [1]. And the changes of electricity consumption in demand side, caused by weather or productive activity [2], require a real-time response from the operation strategy of EGS. Therefore, realizing the flexible control of geothermal power

generation is imperative to ensure orderly power consumption in demand side.

The flexible operation strategy can be derived by the historical or predicted data of network load. Consequently, it is necessary to consider the inverse problem of operation strategy in the quantitative analysis of geothermal power generation. The inverse solution was solved by minimizing the object function using some mathematical method, based on the direct problem [3]. At present, the uncertain analysis has become an interest to heat transfer [4], nondestructive testing [5], hydrogeology and geophysical [6] for long. However, the inverse problem of operation strategy is rarely covered in the investigations of EGS.

EGS is a highly nonlinear and strong coupling system, the heat extraction process commonly involved the seepage flow, heat transfer and mechanical deformation [7]. Although the full-sized scale test is not always available, the numerical simulation can economically and efficiently provide the underlying data for inverse model to meet the estimation of power requirement in demand side. The numerical model can be established based on the real geological data that depend on the geologic investigation, experimental testing, etc. Therefore, the combination of numerical model and inverse method is conducive to managing and optimizing the geothermal power generation. The core of inverse problem is to derive the unknown cause from the known result. Likewise, the local electricity consumption always presents a certain pattern due to the impacts of seasonal reasons, sinusoidally with the time [8], which can be regarded as the known conditions to find an appropriate operation for EGS. The forward method is used to predict and optimize the generating capacity of EGS, and the operation strategies can be obtained by the inverse analysis according to the local market demand. In EGS, once the well layout scheme is determined and reservoir reformation is completed, geothermal generating capacity depends only upon the injection temperature, injection mass flow rate and production pressure. Besides, the injection temperature is often set as constant to avoid the scaling phenomenon in the geothermal industry [9]. Ultimately, the electricity production of EGS is associated with the injection mass flow rate and production pressure. Therefore, how to achieve the flexible control strategy of EGS is the main problem that needs to be solved, according to the response of electricity consumption in a particular area.

In present work, a EGS with pinnate horizontal well was investigated, as shown in Fig. 1. The heat extraction performances have been comprehensively evaluated

from the view of well structure in our previous work [10]. Therefore, the present research objective is to derive the flexible operation strategy of EGS with pinnate horizontal well according to the local power consumption of demand side. The output power characteristics of EGS with pinnate horizontal well are objectively described by the multivariate non-linear regression model. Based on the inverse framework of particle swarm optimization (PSO) with self-adaptive inertia weight, the available operation strategy of EGS is derived. The main contributions can be as follows:(1) A nested iterative program is employed to develop the relationship between the output power capacity of EGS and operation parameters over time. (2) Inverse technique of PSO with self-adaptive inertia weight is utilized to perform identifying analysis on flexible operation strategy. (3) The proposed inverse model fully takes the seasonally uncertain effect of power consumption in demand side on operation strategy into account. (4) A comparative analysis is presented to explore the influence of flexible operation strategy on variation of physical filed within the reservoir.

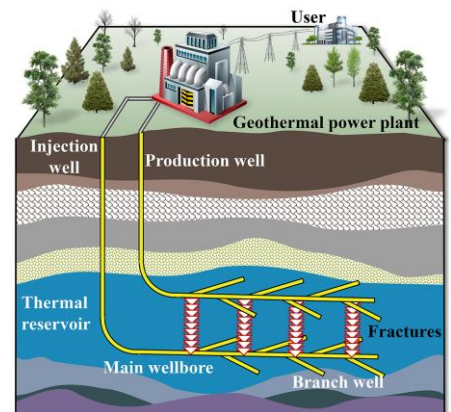


Fig. 1. Schematic of EGS with pinnate horizontal well.

2. MODEL DESCRIPTION

2.1 Model assumption

For convenience in simplifying the calculation process, some reasonable assumptions are made without affecting the whole evaluation. Water is regarded as the geofluid in the heat extraction process, and thermophysical properties of water is shown below. In addition, there is no phase change in the thermal reservoir under the high pressure and high temperature conditions [11]. The fractured reservoir is assumed as homogeneous and isotropic porous medium at the initial conditions. The chemical effects are not considered in the simulation [12]. Local thermal equilibrium method is

used to describe the heat transfer between working fluid and rock matrix [13]. According to the data analysis [8], the electrical load in demand side has a sinusoidally periodicity and regularity.

2.2 Model description

The proposed EGS, simplified as shown in Fig. 2, consists of surrounding rock, a fractured geothermal reservoir, several vertical fractures, one injection well and one production well. In present work, the thermal reservoir, with a size of 500 m × 500 m × 500 m, is situated at a depth of 3500 m~4000 m. The distance from the external surface of surrounding rock to that of thermal reservoir is 100 m. Nine fractures are embedded in the central location of the fractured reservoir with dimension of 350 m × 400 m, the fracture spacing and aperture are 40 m and 1.5 mm. The injection well and production well are drilled at the depth of 3050 m and 3450 m, respectively. Besides, the length of main wellbore and branch well are 300 m and 200 m, respectively. The diameter of operation well is 0.2 m. According to the geological conditions of Qiabuqia geothermal field, the related parameters are summarized in Table 1.

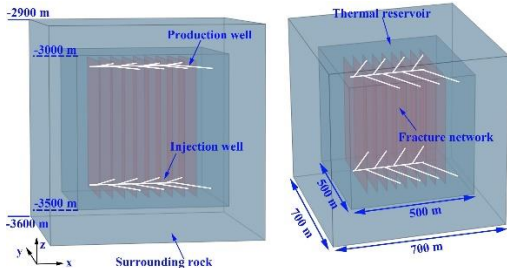


Fig. 2. Physical model of EGS with horizontal well.

Table 1

Geological parameters of numerical model [14-16].

Parameters	Rock reservoir	Fractures
Thermal conductivity	3 W/(m·K)	2.5 W/(m·K)
Density	2700 kg/m ³	2400 kg/m ³
Heat capacity	1000 J/(kg·K)	800 J/(kg·K)
Initial porosity	0.01	0.99
Poisson ratio	0.22	0.22
Biot-Wills coefficient	0.7	0.7
Thermal expansion coefficient	5×10 ⁻⁶ 1/K	-
Elastic modulus	35 GPa	-
Initial aperture	-	0.1 mm
Initial stiffness	-	400 GPa
Maximum closure	-	0.07 mm
Storage coefficient	1×10 ⁻¹⁰ 1/Pa	5×10 ⁻¹⁰ 1/Pa
Initial permeability	5×10 ⁻¹⁵ m ²	-

2.3 Inversion framework

In present work, the whole process of inversion framework is shown in Fig. 3, the detailed description as follows:

1. A series of alternative combinations of decision variables are designed to explore the heat extraction response of EGS with pinnate horizontal well. The estimated results, as represented by their trends and ranges, contains the prior knowledge about the generation capacity of proposed system.

2. Based on the obtained dataset, some key data are extracted and utilized to construct a surrogate model, which can effectively describe the relationship between the operation time, operation strategy and generation capacity. To better perform the regression, a nested iterative program is employed to fit the non-linear curve using the non-linear least squares and Levenberg-Marquardt method. The former is used to explore the relationship between the generation capacity and operation time while the latter is responsible for completing the operation strategy fitting.

3. Combined with the predicted data of power consumption in demand side, the surrogate model is introduced into the self-adaptive inertia weight-based PSO inversion framework. The dynamic inertia weight coefficient (w) is expressed by Eq. (1). The corresponding operation strategy is inferred from the predicted data. Finally, the reliability and accuracy of inversion method

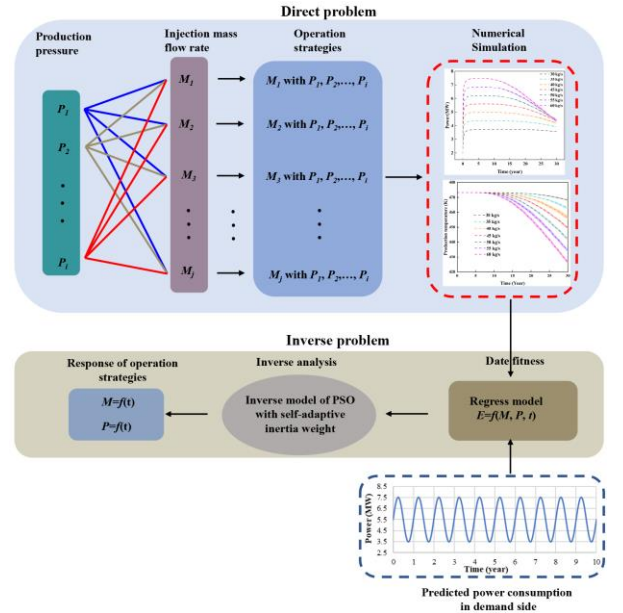


Fig. 3. Schematic of the self-adaptive inertia weight-based inversion framework. The direct model are tested by the direct model.

$$w = \begin{cases} w_{\min} - \frac{(w_{\max} - w_{\min}) \times (f - f_{\min})}{f_{\text{avg}} - f_{\min}}, & f \leq f_{\text{avg}} \\ w_{\max}, & f > f_{\text{avg}} \end{cases} \quad (1)$$

Where w_{min} and w_{max} are the minimum and maximum value of inertia weight coefficient, respectively. f is real-time objective function value, f_{avg} and f_{min} are the average and minimum value of all the particles.

Besides, the output power E_{output} (MW) is employed to evaluate the generation capacity of EGS with pinnate horizontal well, which is expressed as

$$E_{output} = \frac{\eta_{ex} (m_{pro} h_{pro} - m_{inj} h_{inj}) \left(1 - \frac{T_0}{T}\right)}{1000} \quad (2)$$

where η_{ex} represents the exergy efficiency, m is the flow rate, kg/s. h is the enthalpy, kJ/kg. The subscript *pro* and *inj* represent the production well and injection well, respectively.

2.4 Initial and boundary conditions

As for the heat transfer, initial temperature of 473.15 K is set for the whole computational domain and the injection temperature is fixed at 313.15 K, all outer surfaces of the surrounding domain are assumed to be adiabatic. As for the hydraulic conditions, a pore pressure gradient of 0.006 MPa/m is formed in the thermal reservoir after the reconstruction. The top surface of thermal reservoir is assumed to be 30 MPa. Besides, there is no pore pressure in the surrounding rock domain due to its characteristic of low porosity and low permeability. All outer surfaces of the surrounding domain are assumed to be impermeable. To explore the effect of operation strategies on generating capacity, the injection mass flow rate and production pressure vary from 30 kg/s to 60 kg/s and 18 MPa to 22 MPa, respectively. As for the mechanical field, in-situ stresses with 90 MPa, 80 MPa and 70 MPa are applied to the surrounding rock domain in the positive direction of z-axis, y-axis and x-axis, respectively. The boundary conditions of zero displacement are constrained in the negative direction of coordinate axis.

3. RESULTS AND DISCUSSION

To derive the flexible operation strategy of EGS and identify its effect on the heat extraction performance, the discussion mainly involves four parts. In section 3.1, a sensitivity analysis is developed to explore the effect of operation parameters on power generation, thereby obtaining the required datasets. In section 3.2, the surrogate model is established depend on the characteristics of obtained data. In section 3.3, the flexible operation strategy is derived from the power consumption data of demand side based on the surrogate model. In section 3.4, the performance differences of thermal reservoir are comprehensively

revealed under the condition of flexible operation strategy and optimum operation strategy.

3.1 Sensitivity analysis

In present work, 35 cases are simulated to investigate the impact of operation parameters (injection mass flow rate and production pressure) on the production capacity of EGS with pinnate horizontal well. Fig. 4 presents the performance differences of production temperature and output power under the different operation scenarios. Specifically, there are five evaluation datasets in each injection case. The width of the color band reveals the impact of production pressure on evaluation criteria. The wider the color band, the more significant effect on the evaluation criteria, and vice versa. The dash curves represent the average value of evaluation criteria.

High-yield period is defined as the operation duration before thermal breakthrough. Higher injection flow rate leads to larger reduction of production temperature, which significantly shorts the high-yield period. According to the Fig. 4(a), the minimum thermal breakthrough time is about 10 years when the injection mass flow rate ranges from 30 kg/s to 60 kg/s. However, the output power increases with the increase of injection flow rate. The reason is that the total absorbed heat is increased for the low-temperature working fluid with higher flow rate. During the high-yield period, the maximum output power is 7.47 MW, the minimum output power is 3.74 MW. Besides, the obtained data show that the production pressure has a negligible effect on the production temperature and output power. It can be explained as follows. From the Fig. 5, it can be found that the effective compressive stress within the thermal reservoir is slightly increased when production pressure increases. The tensile stress is positive while the compressive stress is negative. The fluid flow channel can't be opened favorably due to the increase of compressive stress.

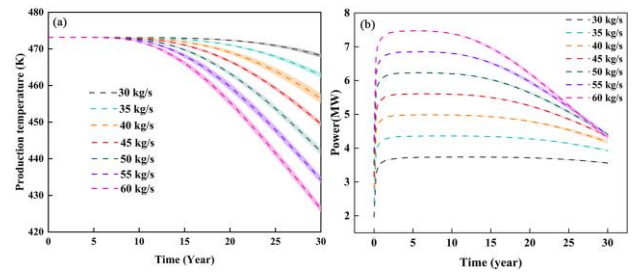


Fig. 4. The evolution of production temperature and power under different operation scenarios.

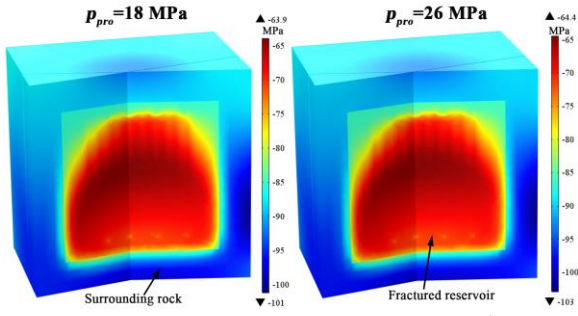


Fig. 5. Effective stress distribution of $m = 60$ kg/s with $p_{pro} = 18$ MPa and $p_{pro} = 26$ MPa at the end of operation.

3.2 The construction of surrogate model

The relationship between the injection flow rate and the output power is predicted with just the high-yield period data in present work. According to the data distribution of output power, the initial function model can be expressed as

$$E(t) = a + b(c - e^{(-t/d)}), 0 \leq t \leq 10 \quad (3)$$

Where E represents the output power. t is time (year). a , b , c and d are function of the injection flow rate, respectively. The non-linear least square is used to solve the undetermined coefficient, the results are shown in Table 2. In addition, Levenberg-Marquardt method is introduced into the nested iterative program to explore the relationship between the undetermined coefficient and injection flow rate. The corresponding expressions are formed as Eq. (11), where m is the injection flow rate.

Table 2

Regression coefficient for a , b , c and d .

Operation conditions	Value			
	a	b	c	d
30 kg/s	-5	1.7418	5.0618	0.2301
35 kg/s	-5.5	1.9678	5.001	0.20259
40 kg/s	-5.7	2.133	4.993	0.18759
45 kg/s	-6.5	2.4168	5.0325	0.18591
50 kg/s	-7.17	2.6743	5.0402	0.18551
55 kg/s	-7.8	2.9235	5.0153	0.18511
60 kg/s	-8.5	3.1862	5.0278	0.18342

$$\begin{aligned}
 a &= -0.11836m - 1.26964 \\
 b &= 0.04847m + 0.25359 \\
 c &= 5 \\
 d &= 0.94056 - 0.04559m \\
 &\quad + 9.11057 \times 10^{-4} m^2 \\
 &\quad - 6.02667 \times 10^{-4} m^3
 \end{aligned} \quad 30 \leq m \leq 60 \quad (4)$$

The indicator of mean absolute deviation is introduced to assess the disagreement between numerical value and predicted value. Four cases are randomly selected to numerically and theoretically calculate the output power within the constraint conditions, respectively. The comparison results are shown in Fig. 6. The surrogate model shows a high calculation accuracy to predict the output power. The results suggest that the surrogate model can be extend to the injection condition at low rate as well.

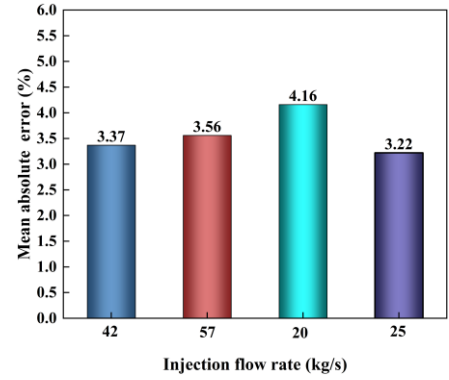


Fig. 6. Accuracy test of surrogate model.

3.3 Operation strategy inversion

In the literature [8], the future electrical load was predicted based on the historical grid data that had the obvious sinusoidal periodicity in the long term. Combined with the output power characteristics of the proposed EGS, the extracted information is used to construct a season-based power consumption pattern for demand side. In present work, summer and winter are considered as the peak season while the spring and autumn are regarded as the low loading season. If the geothermal power plant is fully pressed into service in spring or autumn, the grid load can be described as Eq. (5). Otherwise, the power demand is represented by the Eq. (6). The corresponding generated data are shown in Fig. 7. These synthetic data will be used to derive the operation strategy as the known quantity in inverse model.

Spring or autumn:

$$E_p(t) = 5.4 + 2\sin(4\pi(t - 0.125)) \quad (5)$$

Summer or winter:

$$E_p(t) = 5.4 + 2\sin(4\pi(t - 0.375)) \quad (6)$$

where E_p is the power demand.

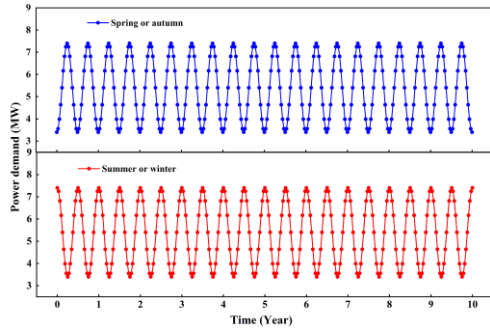


Fig. 7. Power consumption data of demand side in different seasons.

$$\min(|E(m, t) - E_p(t)|) \quad (7)$$

$$s.t. \begin{cases} 0 < m \leq 60 \\ 0 \leq t \leq 10 \end{cases}$$

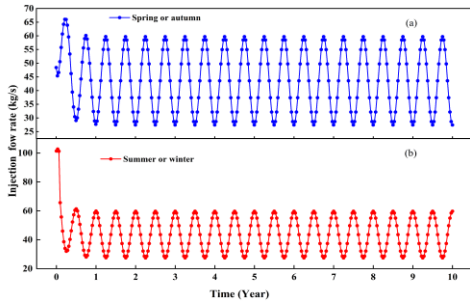


Fig. 8. Inverse estimation of injection flow rate for different

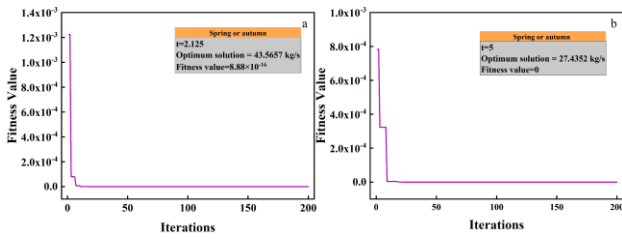


Fig. 9. Variation of fitness value.

Fig. 8 shows the inverse results of injection flow rate for different commissioning seasons. Compared to the Fig. 8(b), the injection flow rate reduces significantly in the early stage if the geothermal power plant is launched

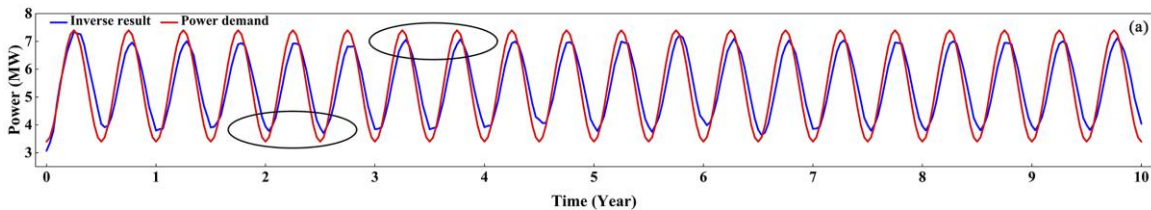


Fig. 10. Comparison of the predicted value and actual demand.

in spring or autumn, which fluctuates sinusoidally in a range of 27.435~59.805 kg/s after one year of operation. However, the injection flow rate will reach to 102.7 kg/s if the geothermal power plant is launched in summer or winter. The high injection flow rate is more likely to

increase the injection pressure, which is directly detrimental to the stability of rock strength. To avoid the geothermally potential seismicity, the geothermal power plant is suggested to be launched in spring or autumn. Besides, Fig. 9 shows that the fitness value is infinitely close to 0 with the increase of iterations. Therefore, the obtained operation strategy by the inverse model is acceptable.

Further, the obtained operation strategy, in the Fig. 8(a), is numerically calculated based on the direct method. The comparison results are shown in Fig. 10. It can be found that there is a time delay between the required power demand and actual output. The time difference is about 11.25 days. The reason is that the working fluid will take a certain amount of time to migrate from the injection well to the production well. Thus, the flexible operation strategy must be implemented early to meet requirement of power for demand side.

3.4 Effect of operation strategy on service performance of thermal reservoir

The geothermal power plant is always demanded to participate in the kurtosis modulation running. Consequently, developing an understanding of the effect of variable and optimum operation strategy on the different physical field within thermal reservoir is crucial. The Non-dominated Sorting Genetic Algorithm II (NSGAI) and the Technique of Order Preference by Similarity to Ideal Solution (TOPSIS) are used to solve the multi-objective problem of operation strategy. The optimization objective is to maximize the accumulative output power and minimize the temperature drop of production well. According to the multi-objective optimization analysis, the Pareto front is presented in Fig. 11. it can be concluded that $\min j=31.8$ kg/s is the optimum operation scheme for the EGS with pinnate horizontal well. At this point, the temperature drop of

production well is predicted as 6.84 K with an accumulative output power of 116.8 MW·a after 30 years of operation.

To explore the effect of flexible operation strategy on the service performance of thermal reservoir, the

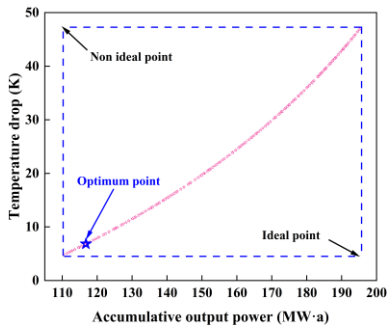


Fig. 11 Pareto frontier for accumulative output power and temperature drop.

results of optimum operation strategy is taken as the reference. Fig. 12 shows that there are two opposing effects, i.e. higher injection flow rate leads to large temperature drop but also slows the thermal breakthrough time. The thermal breakthrough times for optimum and flexible operation strategy are 13.25 years and 14.53 years, respectively. At this point, the cooling region of the thermal reservoir using flexible operation strategy is larger than that with the optimum operation strategy as well, as shown in Fig. 13(a). The larger the effective tensile stress, the wider the fracture aperture, which will enhance the heat convection between working fluid and rock matrix, and vice versa. However, as the injection continues, the increase of effective tensile stress will be reduced in the cooled region due to the existence of geostress, and the opening of fracture is suppressed. It suggests that the flexible operation strategy is beneficial to the alleviation of thermal breakthrough effect, and at the expense of injection pump power, as shown in Fig. 14.

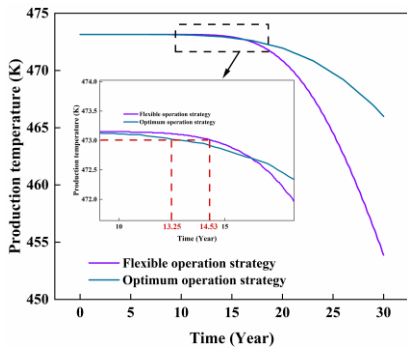


Fig. 12. Comparison of production temperature for different operation strategies.

After the thermal breakthrough, it can be found that the rock permeability and fracture aperture all have an increasing tendency, especially for flexible operation strategy, as shown in Fig. 15 and Fig. 16. The area or volume of increasement region of flexible strategy is larger than that of optimum strategy. The maximum

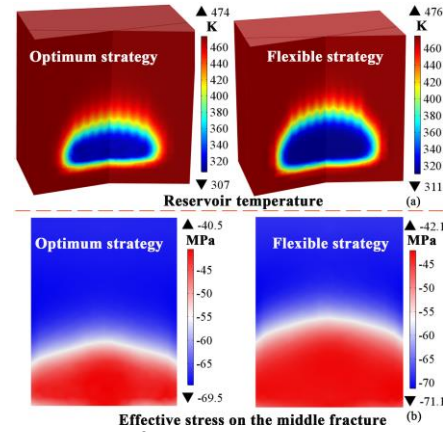


Fig. 13. Comparison of internal characteristics with different operation strategies under the thermal breakthrough moment.

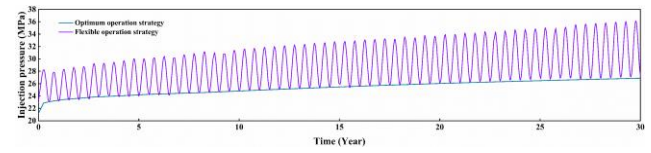


Fig. 14 Comparison of injection pressure for different operation strategies.

difference of rock permeability is 6.8% at reservoir center in year 22.5, as shown in Fig. 17. This is the primary reason for the production deterioration. The flexible operation strategy should be replaced by the optimum operation strategy after the completion of thermal breakthrough to protect the service life of EGS with horizontal well.

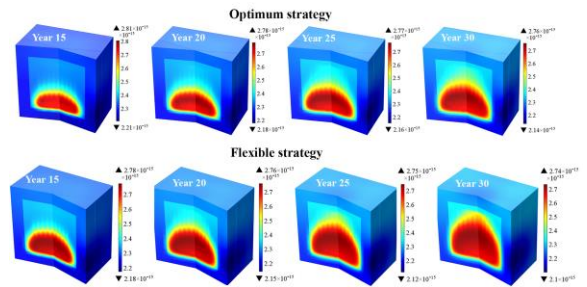


Fig. 15 Comparison of rock permeability for different operation strategies.

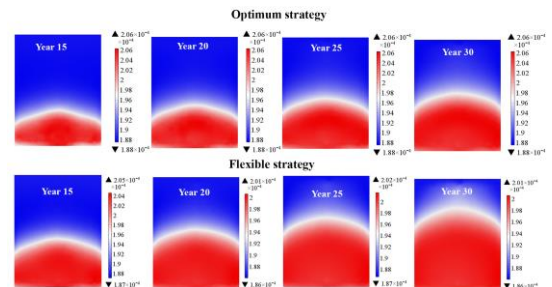


Fig. 16. Comparison of fracture aperture for different operation strategies.

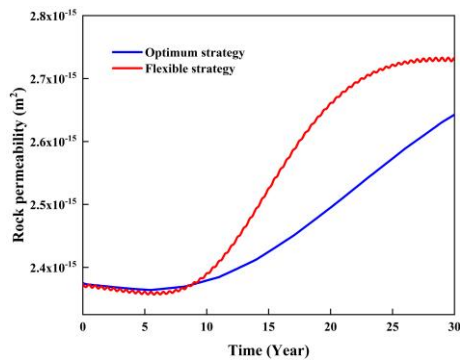


Fig. 17. Comparison of rock permeability for different operation strategies.

4. CONCLUSIONS

A EGS with pinnate horizontal well is proposed for efficient utilization of hot dry rock resources. According to the power consumption in demand side, the flexible operation strategies of EGS are predicted and identified in present work. The main findings of the present work are drawn as follows:

(1) The power generation capacity of EGS is slightly influenced by the production pressure, and is directly proportional to the injection flow rate before the completion of thermal breakthrough. However, the higher the production pressure, the larger the pump consumption in injection well.

(2) Under the current operation conditions, the combination of Levenberg-Marquardt method with PSO with self-adaptive inertia weight inversion algorithm provides an efficient means of characterizing flexible operation strategy of EGS with pinnate horizontal well. The maximum relative error of inverse result is less than 12.3%.

(3) Spring or autumn are the great time for launching geothermal power plant. According to the prediction of power consumption, the flexible operation strategy should be implemented 11.25 days in advance. Compared with the optimum operation strategy, the application of flexible operation strategy delays the thermal breakthrough time of 1.28 years, but needs more injection power.

ACKNOWLEDGEMENT

The authors gratefully acknowledge the financial support provided by the National Key R&D Program of China (No. 2018YFB1501805).

DECLARATION OF INTEREST STATEMENT

The authors declare that they have no known competing financial interests or personal relationships that could

have appeared to influence the work reported in this paper. All authors read and approved the final manuscript.

REFERENCE

- [1] Asai P, Panja P, McLennan J, Moore J. Performance evaluation of enhanced geothermal system (EGS): Surrogate models, sensitivity study and ranking key parameters. *Renewable Energy*. 2018;122:184-95.
- [2] Singh P, Dwivedi P. A novel hybrid model based on neural network and multi-objective optimization for effective load forecast. *Energy*. 2019;182:606-22.
- [3] Gostimirovic M, Sekulic M, Trifunovic M, Madic M, Rodic D. Stability analysis of the inverse heat transfer problem in the optimization of the machining process. *Applied Thermal Engineering*. 2021;195.
- [4] Zálešák M, Charvát P, Klimeš L. Identification of the effective heat capacity–temperature relationship and the phase change hysteresis in PCMs by means of an inverse heat transfer problem solved with metaheuristic methods. *Applied Thermal Engineering*. 2021;197:117392.
- [5] Kou W, Chen L, Sun F, Yang L. Application of bacterial colony chemotaxis optimization algorithm and RBF neural network in thermal NDT/E for the identification of defect parameters. *Applied Mathematical Modelling*. 2011;35:1483-91.
- [6] Jiang Z, Zhang S, Turnadge C, Xu T. Combining autoencoder neural network and Bayesian inversion to estimate heterogeneous permeability distributions in enhanced geothermal reservoir: Model development and verification. *Geothermics*. 2021;97.
- [7] Shi Y, Song X, Song G. Productivity prediction of a multilateral-well geothermal system based on a long short-term memory and multi-layer perceptron combinational neural network. *Applied Energy*. 2021;282:116046.
- [8] Chen Y, Zhang D. Theory-guided deep-learning for electrical load forecasting (TgDLF) via ensemble long short-term memory. *Advances in Applied Energy*. 2021;1:100004.
- [9] Xie J, Wang J, Liu X. The role of fracture networks randomness in thermal utilization of enhanced geothermal system. *International Communications in Heat and Mass Transfer*. 2021;126:105414.
- [10] Xie J, Wang J, Liu X. Performance analysis of pinnate horizontal well in enhanced geothermal system. *Applied Thermal Engineering*. 2022;201:117799.
- [11] Zhou L, Zhu Z, Xie X, Hu Y. Coupled thermal–hydraulic–mechanical model for an enhanced geothermal system and numerical analysis of its heat

mining performance. *Renewable Energy*. 2022;181:1440-58.

[12] Shi Y, Song X, Feng Y. Effects of lateral-well geometries on multilateral-well EGS performance based on a thermal-hydraulic-mechanical coupling model. *Geothermics*. 2021;89.

[13] Li S, Wang S, Tang H. Stimulation mechanism and design of enhanced geothermal systems: A comprehensive review. *Renewable and Sustainable Energy Reviews*. 2022;155:111914.

[14] Liu G, Zhou C, Rao Z, Liao S. Impacts of fracture network geometries on numerical simulation and performance prediction of enhanced geothermal systems. *Renewable Energy*. 2021;171:492-504.

[15] Zhang C, Hu S, Zhang S, Li S, Zhang L, Kong Y, et al. Radiogenic heat production variations in the Gonghe basin, northeastern Tibetan Plateau: Implications for the origin of high-temperature geothermal resources. *Renewable Energy*. 2020;148:284-97.

[16] Lei Z, Zhang Y, Yu Z, Hu Z, Li L, Zhang S, et al. Exploratory research into the enhanced geothermal system power generation project: The Qiabuqia geothermal field, Northwest China. *Renewable Energy*. 2019;139:52-70.